



ARTICLE



Optogenetic inhibition of indirect pathway neurons in the dorsomedial striatum reduces excessive grooming in Sapap3-knockout mice

Kathia I. Ramírez-Armenta¹, Hector Alatraste-León¹, Anil K. Verma-Rodríguez¹, Argelia Llanos-Moreno¹, Josué O. Ramírez-Jarquín¹ and Fatuel Tecuapetla¹  

© The Author(s), under exclusive licence to American College of Neuropsychopharmacology 2021

Excessive grooming of Sapap3-KO mice has been used as a model of obsessive-compulsive disorder (OCD). Previous studies suggest that dysregulation of cortico-striatal circuits is critically important in the generation of compulsive behaviors, and it has been proposed that the alteration in the activity patterns of striatal circuitry underlies the excessive grooming observed in Sapap3-KO mice. To test this hypothesis, we used in-vivo calcium imaging of individual cells to record striatal activity in these animals and optogenetic inhibition to manipulate this activity. We identified striatal neurons that are modulated during grooming behavior and found that their proportion is significantly larger in Sapap3-KO mice compared to wild-type littermates. Inhibition of striatal cells in Sapap3-KO mice increased the number of grooming episodes observed. Remarkably, the specific inhibition of indirect pathway neurons decreased the occurrence of grooming events. Our results indicate that there is striatal neural activity related to excessive grooming engagement in Sapap3-KO mice. We also demonstrate, for the first time, that specific inhibition of striatal indirect pathway neurons reduces this compulsive phenotype, suggesting that treatments that alleviate compulsive symptoms in OCD patients may exert their effects through this specific striatal population.

Neuropsychopharmacology (2022) 47:477–487; <https://doi.org/10.1038/s41386-021-01161-9>

INTRODUCTION

The performance of sequential actions has been linked to the active participation of cortico-basal ganglia-thalamic loops. Disorders that affect these loops result in aberrant phenotypes related to the generation and control of motor behaviors [1–5]. Compulsions are an example of deficits in the control of sequence behaviors and are defined as a series of actions that an individual repeats despite negative consequences. They are a characteristic feature of various disorders and a hallmark symptom of patients diagnosed with obsessive-compulsive disorder (OCD) [6, 7]. Studies with OCD patients have reported morphological alterations in cortico-striatal-thalamic circuits [8–10] and hyperactivation of these regions during symptomatic provocation paradigms. These alterations suggest a key role for these circuits in the generation and regulation of compulsive behaviors [11–13]. Animal models of compulsivity have been used to understand the physiology that underlies compulsive behaviors, often through the quantification of excessive grooming [14–16]. Sapap3-KO mice carry a constitutive deletion of the Sap90/Psd95 associated protein 3 (Dlga3 or Gkap). This protein indirectly participates in the association of glutamatergic receptors in the postsynaptic membrane [15, 17]. Sapap3 expression is found in several brain regions including the neocortex, hippocampus, cerebellum, and striatum, with the highest expression being found in the striatum [18]. Mice lacking this protein display excessive grooming that generates lesions on the face and body

of the animals (construct validity). This is reduced when Sapap3 is reconstituted into the striatum or when mice are treated with fluoxetine (predictive validity) [15, 19, 20].

Experimental evidence has shown that the innate grooming behavior observed in mice is represented in the striatal activity [21, 22]. Repeated optogenetic activation of orbitofrontal cortex (OFC) inputs to the striatum has been shown to generate episodes of excessive grooming in wild-type mice [23]. Consistent with striatal involvement, it has been suggested that a reduction in striatal activity, induced by activation of specific cortical inputs, reduces the excessive grooming phenotype observed in the Sapap3-KO during the presentation of a conditioned stimulus [19]. Furthermore, alterations in the synaptic strength (enhancement or depressing) of anterior cingulate (ACC), OFC, motor (M1) and premotor (M2) cortico-striatal inputs in Sapap3-KO mice have been demonstrated [24, 25]. Additional evidence for involvement of striatal activity in the excessive grooming of Sapap3-KO mice, is an imbalance in basal ganglia subcircuits after in vitro cortico-striatal stimulation [26]. Some authors attribute this imbalance to alterations in mGluR5 signaling [26, 27], a receptor which is highly expressed in the striatum [28, 29]. These findings support the hypothesis that alterations in striatal activity patterns contribute to the generation of compulsive episodes. To test this hypothesis, we examined the contribution of striatal neurons to the generation of compulsions using the excessive grooming behavior observed in the Sapap3-KO. We examined neural activity during the grooming

¹Instituto de Fisiología Celular, Universidad Nacional Autónoma de México, Ciudad Universitaria, CDMX, México. ✉email: fatuel@ifc.unam.mx

behavior by monitoring GCaMP6s transients in freely moving mice. We compared the activity patterns and the proportion of neurons recruited during grooming in mutant and wild-type mice. Furthermore, we tested if optogenetic inhibition of striatal neurons could reduce the compulsive grooming phenotype observed in the Sapap3-KO mice.

METHODS

Experimental model

Animal procedures were carried out according to official standard (NOM-062-ZOO-1999) and approved by the institutional committee for care and use of laboratory animals of the Cell Physiology Institute (Protocol number FTA121-17) at the National Autonomous University of Mexico. Sapap3-KO mice were purchased from Jackson laboratories (B6.129-Dlgap3tm1Gfng/J, Stock No: 008733) and males and females from 2 to 4 months of age were used. Sapap3-KO and SAPAP3^{+/+} littermates were obtained by crossbreeding Sapap3-KO mice with the C57BL/6J line. A2a-Cre Sapap3-KO and D1-Cre Sapap3-KO mice came from the crossbreeding of Sapap3-KO or Sapap3^{+/+} with D1- or A2a-Cre mice. All mice were crossbred for at least 6 generations. The D1- and A2a-Cre mice were donated by Dr. Rui Costa (GENESAT Project [30]). Animals were housed under a cycle of 12 h light/dark (lights on at 6:00 am) with access *ad libitum* to food and water before the beginning of experiments.

Open field and grooming quantification

Subjects were placed in an open-field arena (40 cm × 40 cm × 30 cm) and recorded from above for 30 min at 75 frames per second (fps). Mice were tracked using Bonsai software [31] to obtain the X and Y coordinates of the mouse centroid (Fig. 1A). Grooming behavior was manually assigned and was defined from the moment in which the mice raised their paws, and performed one of the grooming phases described by Aldridge et al. [21], to the point when the paws returned to the ground. The occurrence probability was estimated by dividing a 15 sec period into three 5 s periods (similar to the basal, inhibition and posterior period in the optogenetic manipulation analysis section). Each period was divided into 1 second windows and in each window, we determined whether there were grooming bouts. We then summed the number of windows in each period (the maximum value was 5). The mean of “grooming in the windows” by period was obtained for each mouse. General displacement was determined using MATLAB scripts and was defined by the sum of the Euclidean distances of the mouse centroid between frames. Movement generated during grooming and rearing episodes was subtracted from the total (the frames corresponding to grooming and rearing behavior were removed) so that only the horizontal distance due to locomotor activity was quantified.

Stereotaxic surgery for GCaMP6s expression and lens implantation

Animals were anesthetized using isoflurane 1–2% and unilaterally injected with 600 nL of GCaMP6s [AAV1.Syn.GCaMP6s.WPRE.SV40 (Addgene #100845-AAV1), Titer: >1 × 10¹³ vg/ml, diluted 1:8] into the DMS using the following coordinates from Bregma (mm), AP: 0.3, ML: 1.8, DV: 2.3–2.4. Injections were performed with glass pipettes using pulses of 9.2 nL every 5 s in slow mode (Nanoject II, Drummond Scientific). One week after virus injections, an endoscope (Lens Probe, 0.5 mm diameter, –8.4 mm, Q < 0.25, Inscopix) was implanted 100 microns above the injection site and fixed to the skull using acrylic resin (Lang Dental Manufacturing, Co.). Two to three weeks post-injection, the miniscope-baseplate was attached (GU091, LabMaker UG).

Acquisition of GCaMP calcium events during grooming behavior in freely moving mice

Starting 3 days post-surgery, mice were habituated to the experimenter for 2–7 days (15 min handling/ day) and to the cable/ miniscope for a further day (20 min). Calcium acquisition was performed using a wide-field fluorescence miniscope (Miniscope, LabMaker UG, [32]), in freely moving mice, at 10 Hz (31 ± 1.8 min sessions for 2.9 ± 0.4 consecutive days). Grooming bouts were manually assigned offline using videos recorded from below at 40 fps in a clear acrylic arena (20 cm × 30 cm × 25 cm; see grooming estimation). Given that both videos were acquired by the same computer, we saved the timestamp of each frame and used it for

alignment. Grooming was manually scored and was aligned to the imaging video by finding the frame of the miniscope video nearest to the start of grooming episodes. Since the behavioral video was acquired at a higher frame rate, the maximum alignment error between both videos was 50 ms (mean: 0.55 ms ± 0.09).

Analysis of GCaMP calcium events

Raw videos were corrected for movement using the TurboReg-ImageJ-plugin [33, 34]. Regions of interest (ROIs) were assigned using the algorithm reported by Lu et al. [35]. The dF/F signals were transformed into deconvoluted neuronal activity using the constrained-foopsi method [36]. To evaluate if there was a difference in striatal activity, we analyzed the amplitude of the peaks and the cumulative events of the deconvoluted signals using the “findpeaks” function in Matlab (we did not use inferred spikes in Fig. 2 since this required the removal of small amplitude events [32]). In Fig. 2 we used the data of three consecutive sessions for each subject, using the algorithm reported by Sheintuch et al. [37] (Supplementary Table 2). To track neurons across sessions, we verified that the neurons only appeared once in our database (we prioritized finding the best sessions that had the largest number of grooming bouts and the largest number of cells. Finding these best sessions, we included that session plus two sessions before for each animal). Supplementary Table 2 shows which sessions were included in each GCaMP figure. For the correction of the decay in signal, we used the automatic correction performed by the MIN1PIPE algorithm [35], nonetheless the percentage of decay for each session is shown in Supplementary Fig. 1. To address if we could include more than one session, we verify if their distribution of the amplitude events in the first vs. the third session was different. Despite tendencies no statistical differences were found (Supplementary Fig. 1B; *p* > 0.05, Kolmogorov-Smirnov). The difference on the number of cells between groups was corrected by down sampling the Sapap3^{+/+} group running 1000 permutations. To evaluate the striatal activity related to grooming behavior, we used one session per subject (the session with the largest number of grooming events). The calcium signal z-score was aligned to grooming onset. To define a modulated cell, the mean of the basal period (–6 to –2 s; this period was selected as some events showed an increase before zero) and grooming period (0–4 s) for each event was calculated, then a Wilcoxon test between these variables was applied. The positive or negative trend was used to define a cell as up or down modulated. A series of grooming bouts (GS) was defined as a set of consecutive grooming bouts with inter-event intervals of less than 3 s. To compare the activity in this GS between groups, the calcium events of modulated cells were calculated by series and the mean frequency was reported.

Stereotaxic surgeries for optogenetic inhibition

Subjects were anesthetized using 1–2% isoflurane and 500 nL volumes of viral vector (for striatal inhibition: AAV5-hSyn-eArch3.0-eYFP or AAV5-hSyn-eYFP, titer >10¹² vg/mL; for striatal pathway inhibition: AAV5-EF1a-DIO-eArch3.0-eYFP or AAV2-EF1a-DIO-eYFP, titer: >10¹² vg/mL, UNC Vector Core) were injected bilaterally into the DMS using the same coordinates and injection procedures as for GCaMP. Optical fibers (300 μm diameter, ~3.0 mm length) were implanted 100 microns above the injection sites and fixed to the skull using acrylic resin (Lang Dental Manufacturing, Co.).

Optogenetic inhibition

To evaluate the effects of optogenetic inhibition on grooming and motor activity, mice were placed in an open field arena (40 cm × 40 cm × 30 cm) and a continuous light pulse was delivered for 5 s every 35 s (18–20 mW, 550 nm, 15 pulses). The inhibition period was divided into 1 second windows and binarily assigned if there were grooming bouts in those windows (Fig. 4A). The sum of the windows was calculated for the inhibition period and 5 seconds periods before and after the inhibition. The mean of the evaluated window from all pulses of light was obtained for each mouse. The grooming index was quantified by dividing the mean number of grooming windows during the inhibition period (or during the posterior 5 s period) by the mean of grooming windows in the basal period for each subject. The occurrence probability was estimated by binarily quantifying if there was grooming in 1 s windows during 15 s periods (5 s of inhibition + 5 s before and after) at 0.02 Hz (this was the frequency of presenting light inhibition), on average in 15 trials per animal. The 15 s window was normalized to the 5 s before the inhibition pulse. Horizontal

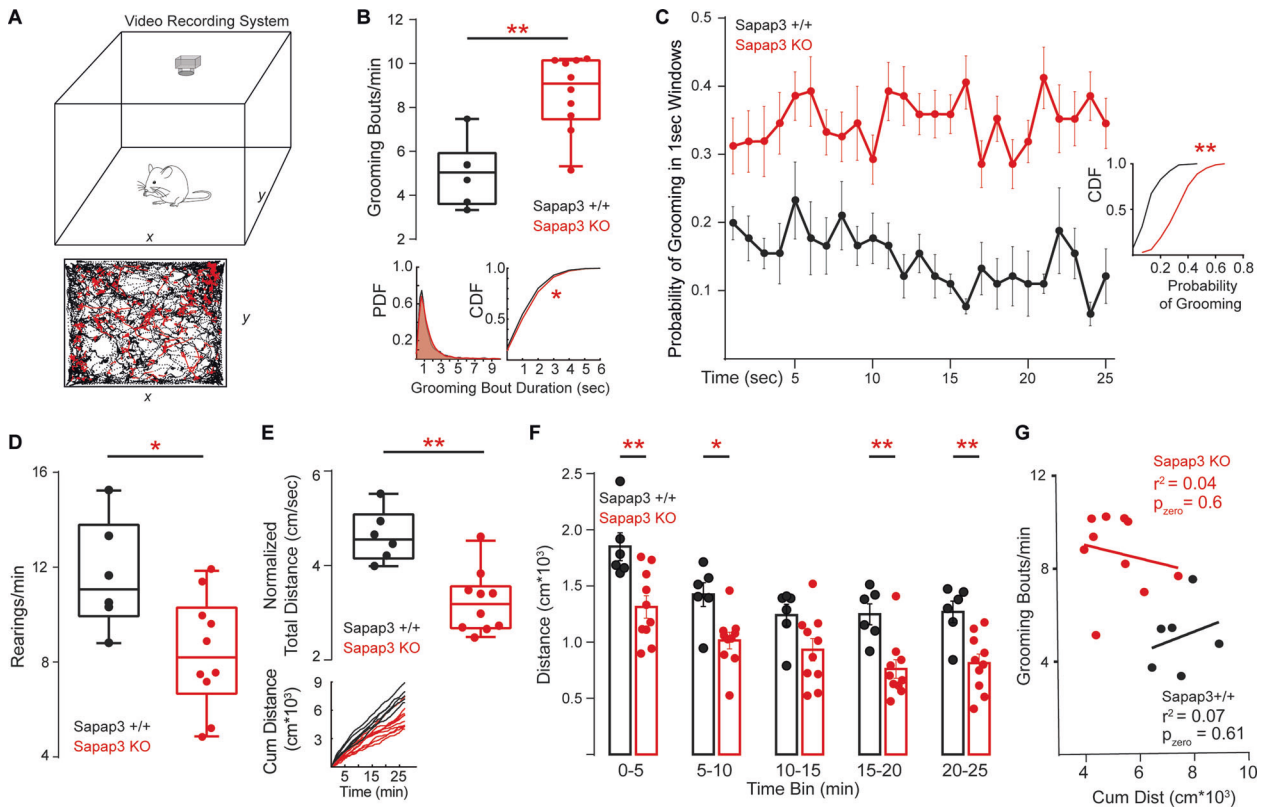


Fig. 1 Sapap3-KO mice show excessive grooming and decreased locomotion. **A** Schematic diagram of the open field setup, the inset is a representative example of mouse tracking, red dots indicate grooming periods. **B** Upper Panel: Grooming bouts per minute (Red: Sapap3-KO: $n = 10$; Black: Sapap3^{+/+}: $n = 6$; Mann-Whitney U, $p < 0.01$). Bottom Panels: Probability and Cumulative density function (PDF and CDF) for grooming bout duration (Kolmogorov-Smirnov test $p < 0.05$) **C** Left Panel: Probability of grooming in 1 s windows in a 15 s period. Right Panel: Cumulative density function (CDF) for the probability of grooming in 1 s windows from the data on the left (Kolmogorov-Smirnov test, $p < 0.01$). **D** Rearing events per minute (Mann-Whitney U, $p < 0.05$). **E** Total distance normalized to the session duration (Mann-Whitney test $p < 0.01$), inset cumulative distance for each subject, movement related to periods of grooming and rearing activity was subtracted. **F** Quantification of total distance for each 5 min block across the session (Mann-Whitney U for each block, * $p < 0.05$ and ** $p < 0.01$). **G** Correlation between cumulative distance and grooming bouts per minute (Sapap3^{+/+} R: 0.07, $p = 0.61$. Sapap3-KO, R 0.04, $p = 0.6$).

displacement was determined as described before and was quantified in 1 s windows and normalized to 1 s before the start of the light pulse. A fixed threshold related to the mean rate of movement before the light pulse was used to classify trials as slow or fast (light was delivered when the animals were at rest/slow or fast moving respectively, Supplementary Fig. 2). The movement index was the ratio of the horizontal displacement mean during the 5 s of light and the horizontal displacement in the 1 s window before the inhibition.

Electrophysiological recordings

To corroborate the inhibition of striatal activity 600 nL of Syn-Arch3.0 was injected into the DMS of one Sapap3-KO mouse. Three weeks after the injection, an optrode: mobile electrode array (16 microwire bundles, Innovative Neurophysiology Inc.) coupled with a custom-made optical fiber (200 μm diameter, ThorLabs, Inc) was placed 100 μm above the injection site. One week later the subject was placed in the open field arena and the inhibition protocol was applied while performing electrophysiological recordings for one session per day. Three sessions were used for our analysis; the dorsoventral positions were -2.3 nm, -2.45 nm, and -2.5 nm, respectively. The recording data was acquired at 30 kHz and passed through a 750 Hz filter (CerePlex Direct, Blackrock Microsystems). Units were manually sorted using the Offline Sorter Software (Plexon, Inc). To define modulated cells, we aligned activity to the onset of the 15 light pulses and calculated peri event-histograms for each unit (100 ms fixed windows). The Kruskal-Wallis test was used to compare the distribution of 3 s before the light pulse and the distribution during the 5 s pulse. A second criterion (latency) was applied to significantly modulated units, and only included neurons in which the distribution of the first second of the light pulse was different to the 3 s before the pulse.

Statistical analysis

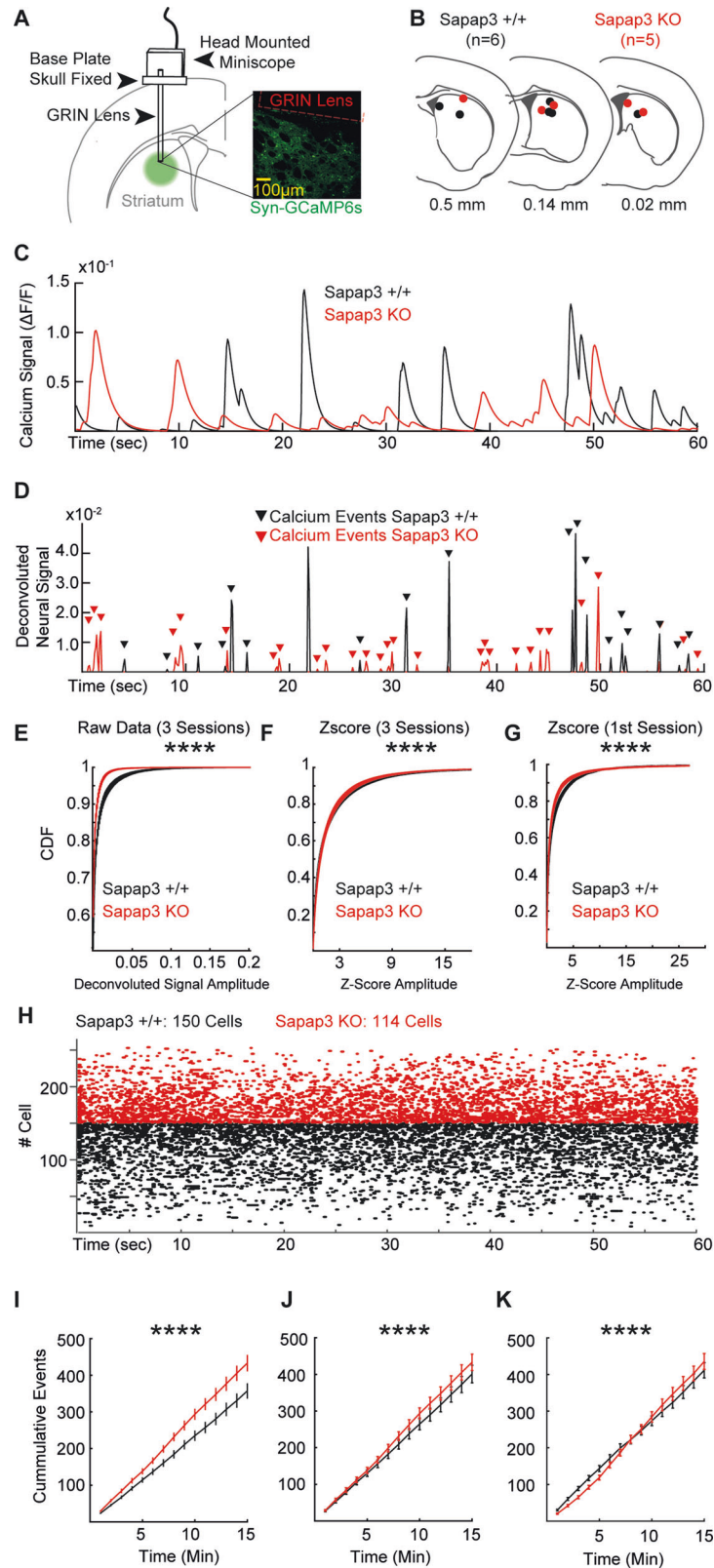
All data were presented as mean \pm SEM unless otherwise specified in the text. The significance level was $p < 0.05$. The Chi-square test was used to compared proportions and the Wilcoxon test was applied to paired comparisons. For non-paired comparisons, the Mann-Whitney U test was used. For group comparisons across time periods, two-way ANOVA/Sidak tests were used. All statistical analyses were done using GraphPad Prism 6.01 and MATLAB R2020a.

RESULTS

Three experiments were conducted to establish the contribution of the striatum to the generation of excessive grooming, a model of compulsions. First, we confirmed the compulsive grooming phenotype and reduction of locomotion in Sapap3-KO mice. Second, through calcium imaging we recorded striatal activity in Sapap3-KO mice and their littermates, Sapap3^{+/+}. Third, we evaluated the effects of optogenetic inhibition of striatal activity on the generation of excessive grooming in Sapap3-KO mice.

Sapap3-KO mice display excessive grooming and decreased locomotion

The presence of excessive grooming in the Sapap3-KO has been used as model to study compulsions [19, 38, 39]. To validate the presence of excessive grooming in the Sapap3-KO we measured the grooming and locomotion of these mice in the open field (Fig. 1A). As previously described, Sapap3-KO mice showed a larger number of grooming bouts (GB) per minute (Fig. 1B, Upper



panel; Mann–Whitney U test $p < 0.01$), with longer durations, when compared to control littermates (Fig. 1B, Bottom panel; Kolmogorov–Smirnov test $p < 0.05$). To further characterize the repetitive grooming, the likelihood of observing it was measured by estimating the probability of finding grooming episodes on a

second-by-second basis. We confirmed the exacerbation of grooming behavior in Sapap3-KO mice by comparing the cumulative distribution of probabilities (CDF) found in each group (Fig. 1C, Right panel; Kolmogorov–Smirnov test $p < 0.01$). Rearing was also found to be decreased in the Sapap3-KO (Fig. 1D,

Fig. 2 Sapap3-KO mice have smaller GCaMP events. **A** Schematic diagram of GCaMP6s infection, lens localization in DMS and head mounted miniscope. **B** Representative diagram for the localization of GRIN lens in the DMS for each group (Black: Sapap3^{+/+} $n = 6$, Red: Sapap3-KO $n = 5$). **C** Calcium signal ($\Delta F/F$) of one representative cell for each group. **D** Deconvoluted neural signal for the calcium traces in (**C**), triangles represent the events detected. **E** Cumulative distribution function (CDF) from the deconvoluted neural signal amplitude of calcium events (Black: Sapap3^{+/+} 114 cells (6 mice), Red: Sapap3-KO 114 cells (5 mice), data collected from 3 sessions per animal. **F** CDF using the Z-Score data from (**E**). **G** CDF using the Z-Score from the first session of each subject (Black: Sapap3^{+/+}: 88 cells, Red: Sapap3-KO 88 cells), (**E–G**): ****Kolmogorov-Smirnov, $p < 0.0001$). **H** Raster plot of calcium events in a representative period of time for all cells [a period of 60 s for all cells (arbitrarily selected) is presented; Black: Sapap3^{+/+} 150 cells (6 mice), Red: Sapap3-KO 114 cells (5 mice)]. For better visualization, the Sapap3^{+/+} (bottom) and Sapap3-KO (top) cells are sorted ascendent and descendent respectively. **I** Cumulative events across time from the data of (**E**). **J** Same as I for the data in (**F**). **K** Same as I for the data in G (I–K): **** Two-Way ANOVA, $p < 0.0001$). In (**E–G**) and (**I–K**), the data were down sampled to equal the Sapap3 KO cells, a representative example was show.

Mann–Whitney U test, $p < 0.05$). Previous studies have reported a reduction in the locomotor activity of Sapap3-KO mice [39], but its phenotype remains unclear [15, 25, 40]. We measured horizontal locomotion and observing a substantial reduction in Sapap3-KO mice compared to controls (Fig. 1E, Mann–Whitney U test $p < 0.01$). To access if this reduction could be seen throughout the session, we measured horizontal locomotion in 5 min blocks and found a decrease in Sapap3-KO mice across the whole session (Fig. 1F, Mann–Whitney U test, $p < 0.05$). To evaluate if the reduction in locomotor activity was related to the increased grooming, we looked to see if the two parameters were correlated but found that they were not (Fig. 1G, Supplementary Table 1).

These results confirm the excessive grooming and decreased locomotion in the Sapap3-KO model.

Sapap3-KO mice show a higher frequency of small calcium GCaMP6s events in striatal cells

Previous work has implicated striatal activity in the generation of compulsive behavior [12, 13, 19, 23]. However, only one study has directly measured striatal activity related to compulsions in the Sapap3-KO model, and suggested a hyperactivation during evoked compulsions [19]. Therefore, we further characterized striatal activity in the Sapap3-KO model by recording calcium transients in the dorsomedial striatum (DMS). This was achieved through GCaMP6s expression which was visualized using micro-endoscopes (Fig. 2A, B), while animals were in the open field. The calcium signal (dF/F ; Fig. 2C) and the deconvoluted neuronal signal (Fig. 2D) were obtained from individual cells. The cumulative distributions (CDF) of the deconvoluted signal amplitudes of the calcium events showed a larger proportion of smaller amplitude events in Sapap3-KO mice compared to controls (Fig. 2E, Kolmogorov-Smirnov Test $p < 0.0001$; Supplementary Table 1). The same finding remains when the deconvoluted signal was normalized to Z-Score or when analyzing the Z-score of the first recording session for each subject (Fig. 2F and G, Kolmogorov-Smirnov Test $p < 0.0001$). Importantly, the Sapap3-KO mice showed a higher number of cumulative events over time, when compared to their control littermates (Fig. 2I–K, Two-Way ANOVA, $p < 0.0001$). The Sapap3^{+/+} cells were down sampled to equal the number of Sapap3 KO and for those animals were more than session was used, we verified that the amplitudes do not differ between sessions (see methods and Supplementary Fig. 1).

Overall, quantification of the amplitude and frequency of the deconvoluted activity of striatal calcium transients showed a higher number of cumulative calcium events along time with smaller amplitudes in Sapap3-KO mice.

The proportion of striatal neurons related to grooming behavior is increased in Sapap3-ko mice

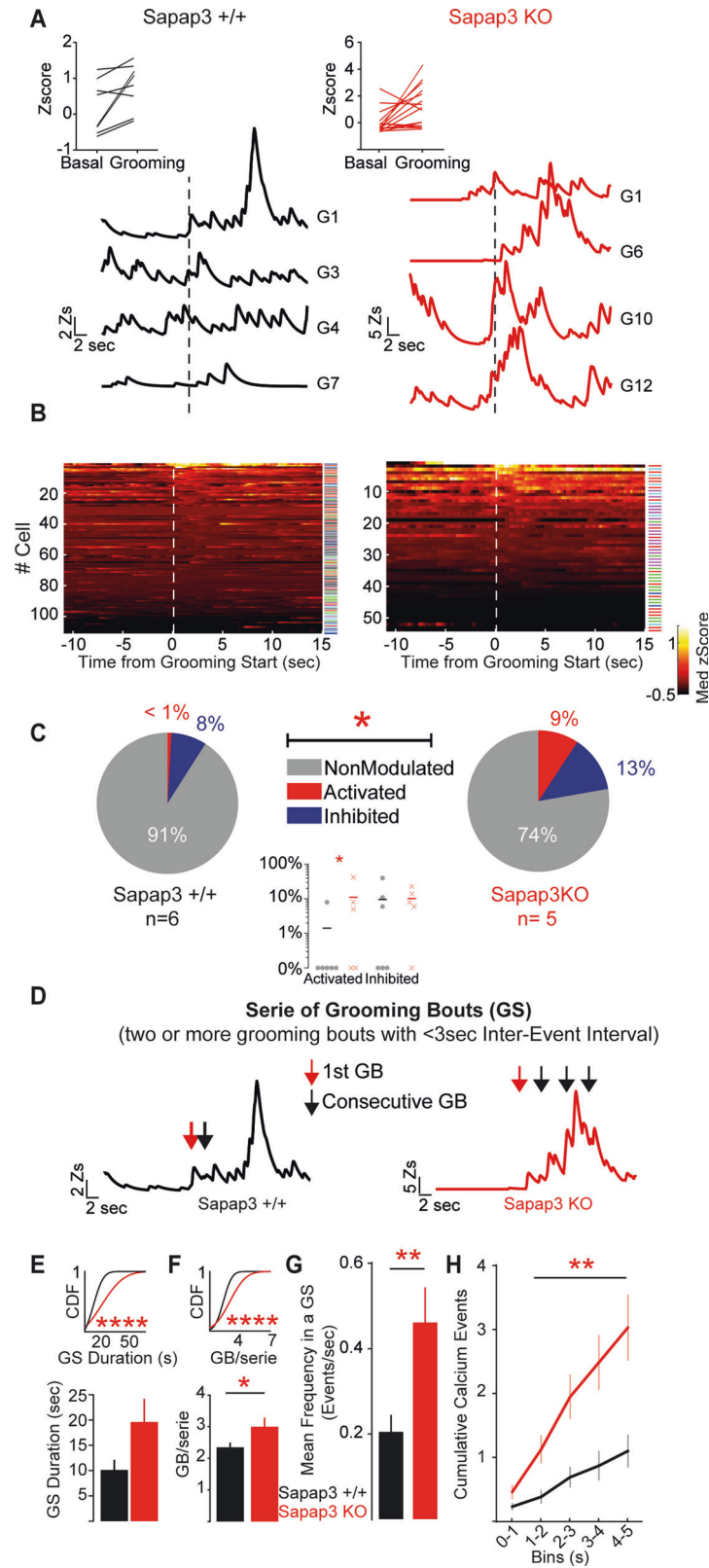
The motor control of innate and stereotyped grooming behavior has been linked to the activity of striatal neurons [22, 41, 42]. To assess if there was an alteration in the striatal activity of Sapap3-KO mice, where grooming behavior is excessive, we aligned the calcium signal to the onset of grooming episodes (Fig. 3A, B). This alignment identified striatal cells in which GCaMP transients were

modulated at grooming onset (Fig. 3B). Remarkably, Sapap3-KO mice showed a larger proportion of modulated cells than littermate controls (Fig. 3C, Sapap3-KO activated: 5/54 cells, inhibited: 7/54 cells; Sapap3^{+/+} activated: 1/111 cells, inhibited 9/111 cells; Chi-square $p < 0.05$). We compared the proportion of activated and inhibited cells separately, but only the proportion of activated cells was found to be significantly different (Fig. 3C: inset; Fisher's test $p < 0.05$). Since a proportion of grooming events repeated before 15 s the comparison of modulated cells was re-evaluated excluding the grooming that overlapped in the basal period, as a result we observed that the larger proportion of modulated cells in the Sapap3-KO mice sustained the tendency (Chi-square $p = 0.17$; data not shown). Nevertheless, when we added two Sapap3 KO where only the striatal medium spiny neurons were marked with the calcium indicator (1 D1 Cre and 1 A2A Cre) and removing the overlapping grooming, we corroborated the higher proportion of grooming related cell in Sapap3-KO animals (Sapap3-KO activated: 8/68 cells, inhibited: 4/68 vs. Sapap3^{+/+}: activated: 2/111 cells, inhibited: 8/111 cells; Chi-square < 0.01 ; data not shown). Furthermore, we observed an accumulation of calcium transients after grooming onset in Sapap3-KO mice (Fig. 3D), so we analyzed series of grooming bouts (GS; a grooming series was defined as a group of consecutive grooming bouts with less than 3 s intervals between events). To analyze the activity patterns of GS, we used the calcium events of the modulated cells for all grooming series (including all calcium transients detected from the non Cre animals). The GS of Sapap3-KO mice had longer durations that control littermates (Fig. 3E bottom panel, Mann–Whitney U, $p > 0.05$; upper panel, Kolmogorov Smirnov, $p < 0.0001$), and contained more grooming bouts (Fig. 3F bottom panel, U-Mann–Whitney $p < 0.05$; upper panel, Kolmogorov Smirnov, $p < 0.0001$). Consistent with the idea of enhanced striatal activity in Sapap3-KO mice during compulsions [19], we observed a higher frequency of calcium events during the series of grooming bouts in the modulated cells of these animals when compared to control littermates (Fig. 3G, Mann–Whitney U, $p < 0.01$). This effect was also observed when events were divided into 1 s bins across the series duration (Fig. 3H, Mann–Whitney U, $p < 0.01$).

Together these observations, along with the increase in the proportion of modulated cells, suggest that an increase in DMS activity could underly the excessive grooming phenotype observed in the Sapap3-KO.

Inhibition of striatal cells increases grooming behavior in Sapap3-Ko mice

Given the increased proportion of cells related to grooming onset in the Sapap3-KO and the enhanced striatal activity during grooming, we hypothesized that a reduction in striatal activity in these mice could diminish their compulsive phenotype. To test this hypothesis, we carried out a series of experiments to optogenetically inhibit either general striatal activity, or the activity of specific projections neurons, while evaluating the probability of grooming. Optogenetic inhibition of general striatal activity was achieved by expressing archeorodhopsin3.0 (Arch3.0-eYFP; using the synapsin



promoter) and implanting optical fibers into the DMS of Sapap3-KO mice (Fig. 4A, B). We proved the effectiveness of our optogenetic inhibition protocol to reduce striatal activity by performing in vivo electrophysiological recordings in the DMS of Sapap3 KO mice (Fig. 4C). Surprisingly, and contrary to our

hypothesis, general inhibition of striatal neurons in the DMS increased the grooming phenotype (Fig. 4D, Friedman Test $p < 0.01$, Dunn's multiple comparison $p < 0.05$). This effect was seen only in the general inhibition of Sapap3-KO animals, and not in Sapap3-KO mice expressing only eYFP, or in C57BL/6 mice

Fig. 3 The proportion of striatal neurons related to grooming behavior is increased in Sapap3-KO mice. **A** Representative examples of calcium transients during different grooming events for one modulated cell from each group. The insets show the paired comparison between the basal mean activity vs. the grooming mean activity for each grooming event recorded, the method used to classify cells as modulated. **B** Color map for striatal neurons aligned to grooming onset for each group (median z-score). The color code column on the right side of each panel illustrates to which animal it belongs. **C** Proportion of modulated cells (Sapap3^{+/+} Negatively Modulated: 9 Cells, Positively Modulated: 1 Cell, non-Modulated: 101 Cells; Sapap3-KO Negatively Modulated: 7 Cells, Positively Modulated: 5 Cells, non-Modulated: 42 Cells; Chi-square, $p < 0.05$). Inset in the middle: Individual proportions of modulated cells (Black: Sapap3^{+/+} (6 mice), Red: Sapap3-KO (5 mice)). Every point is an animal, the horizontal lines are the mean of each group. Activated Comparison $p < 0.05$, Inhibited Comparison $p > 0.05$, Fisher test). **D** Time representation of an example of the calcium activity during a series of grooming bouts, red arrows indicate the first grooming bout in the series, black arrows indicate the consecutive bouts (Inter-grooming interval < 3 s) for each group. **E** Grooming Series duration (Sapap3-KO: $n = 19$ GS, Sapap3^{+/+}: $n = 20$ GS; Mann–Whitney U, $p > 0.05$). Insets represent the cumulative distribution function for grooming series duration (Kolmogorov Smirnov test, $p < 0.0001$). **F** Grooming Bouts by Serie (U-Mann–Whitney, $p < 0.05$). Insets represent the cumulative distribution function for grooming bouts by series (Kolmogorov Smirnov test, $p < 0.0001$). **G** Mean frequency in each grooming series for modulated cells (Mann–Whitney U, $p < 0.01$). **H** Cumulative calcium events during grooming series in 1 s bins (Mann–Whitney U, $p < 0.01$).

expressing Arch (Fig. 4D Center and Right Panel; Friedman Test $p > 0.05$, Dunn's multiple comparison $p > 0.05$). The increase was also observed when we compared the ratio of 5 s windows with grooming episodes (on/off) in the Sapap3-KO Arch group with the eYFP or C57BL/6 groups (Fig. 4E, Kruskal–Wallis $p < 0.01$, Dunn's multiple comparison $p < 0.05$). To further confirm this effect, we measured the probability of grooming windows and found a significant increase during the last 3 s of the inhibition pulse (Fig. 4F, Two-way ANOVA $p < 0.0001$).

The effect of optogenetic inhibition on locomotion (horizontal displacement) was also evaluated (Fig. 4G). Sapap3-KO Arch mice showed a reduction in displacement during light inhibition when compared with Sapap3-KO mice expressing only eYFP (Fig. 4H, Two-way ANOVA $p < 0.05$).

Specific inhibition of striatal indirect pathway neurons decreases excessive grooming in Sapap3-Ko mice

Before concluding that inhibition of striatal activity does not decrease grooming in Sapap3-KO mice, and given that the striatum is a highly heterogeneous structure, we asked if specific inhibition of its most prominent cell types—striatonigral (dMSN) or striatopallidal (iMSN) medium spiny projection neurons—would have the same effect. To do this, we crossbred Sapap3-KO mice with either D1-Cre or A2A-Cre mice (these Cre lines specifically target Cre recombinase expression to dMSN or iMSN neurons, respectively [26]). Then we expressed Arch3.0-eYFP in these animals, allowing us to selectively inhibit direct or indirect pathway striatal neurons in Sapap3-KO mice (Fig. 5A, B). We found that inhibition of iMSNs in Sapap3-KO mice decreased grooming episodes during the inhibition pulse (Fig. 5C, Friedman Test $p < 0.01$, Dunn's multiple comparison $p < 0.01$ and ratio on/off: Fig. 5D left panel, Kruskal–Wallis $p < 0.01$, Dunn's multiple comparison $p < 0.05$). This was not observed in Sapap3-KO D1-Cre/A2A-Cre mice expressing only eYFP, or in Sapap3-KO D1-Cre Arch mice (Fig. 5C center and right panels, Friedman Test $p > 0.05$; Dunn's multiple comparison $p > 0.05$), suggesting specific regulation of grooming behavior by indirect pathway striatal projection neurons. Interestingly, an increment of grooming bouts after the direct pathway's inhibition was observed (Fig. 5D Right panel, Kruskal–Wallis $p < 0.05$, Dunn's multiple comparison $p < 0.05$). These differential effects between the inhibition of the pathways were confirmed when the probability of grooming windows was calculated (Fig. 5E, Two-way ANOVA, $p < 0.01$).

We also looked at the effects of specific optogenetic inhibition of direct and indirect pathway neurons in Sapap3-KO mice on locomotion (horizontal displacement) and found that inhibition of either of the pathway resulted in increased locomotor activity (Fig. 5F, Left panel, Mann–Whitney U, $p < 0.05$).

Strikingly, inhibition of direct pathway neurons in Sapap3-KO mice resulted in a strong increase in the movement index (ratio of the 5 s on/5 s off) when animals were at rest or moving slowly (inset in the Fig. 5F slow trials panel, Mann–Whitney U, $p < 0.05$),

differing from what was expected [43–45]. Suspecting that this finding might be a consequence of Sapap3 protein deletion, we inhibited dMSNs or iMSNs in the same striatal region of wild-type mice (C57BL/6 crossbred with the A2a-Cre or D1-Cre lines; Fig. 5G filled bars). Comparison of the movement indices in wild-type and Sapap3-KO animals indicated that it is an impairment in the direct pathway which leads to changes in horizontal displacement in Sapap3-KO mice (Fig. 5G blue bars comparison; Mann–Whitney U, $p < 0.05$).

Together, the results from the optogenetic inhibition of neurons in specific striatal pathways in the Sapap3-KO model show that inhibition of indirect pathway neurons decreases excessive grooming, whilst the inhibition of either indirect or direct pathway neurons increases locomotion. The inhibition of the direct pathway neurons in the Sapap3 KO mice reveal an unexpected role for them in the control of locomotion in this model.

DISCUSSION

In the present study, we used excessive grooming behavior as an approach to study the contribution of striatal circuits to the generation of compulsions. The increased grooming phenotype reported previously in the Sapap3-KO model was confirmed [15, 19, 20, 46]. Our study also shows that the average duration of a bout is longer in the Sapap3 KO.

Several studies have evaluated the effects of Sapap3 protein deletion on locomotion, with contradictory results [15, 25, 47]. We observed a clear reduction in locomotion, but this effect was not correlated with the intensity of grooming. This lack of correlation between grooming and other behaviors has been reported previously for grooming and anxiety [46, 47], as well as grooming and performance in operant conditioning [46], which supports the idea that independent mechanisms govern these phenomena.

We performed single-cell calcium recordings of striatal activity in freely moving Sapap3-KO mice and observed that calcium signals were smaller in amplitude than in control littermates. This corroborates in-vitro findings, which suggest an alteration in postsynaptic currents on MSNs mediated by AMPAR in Sapap3-KO mice after cortical stimulation [15, 25, 48, 49]. In this study, we aimed to target the posterior striatum (based on Matamales et al. 2016, the range of anatomical coordinates that covers the posterior striatum is 0.5 mm to -1.5 mm [50]), since it has been associated with behavioral flexibility and the transition from goal-directed to habitual behaviors [51, 52]. Besides receiving OFC and M2 inputs which have been implicated in the expression of compulsions [8–10].

The proportion of neurons modulated during the onset and maintenance of grooming was larger in Sapap3-KO than control mice. This is in line with several studies reporting activity modulation in several brain regions, including the caudate nucleus, during symptomatic provocation protocols in OCD patients [8, 9, 53]. For example, activation of the caudate nucleus

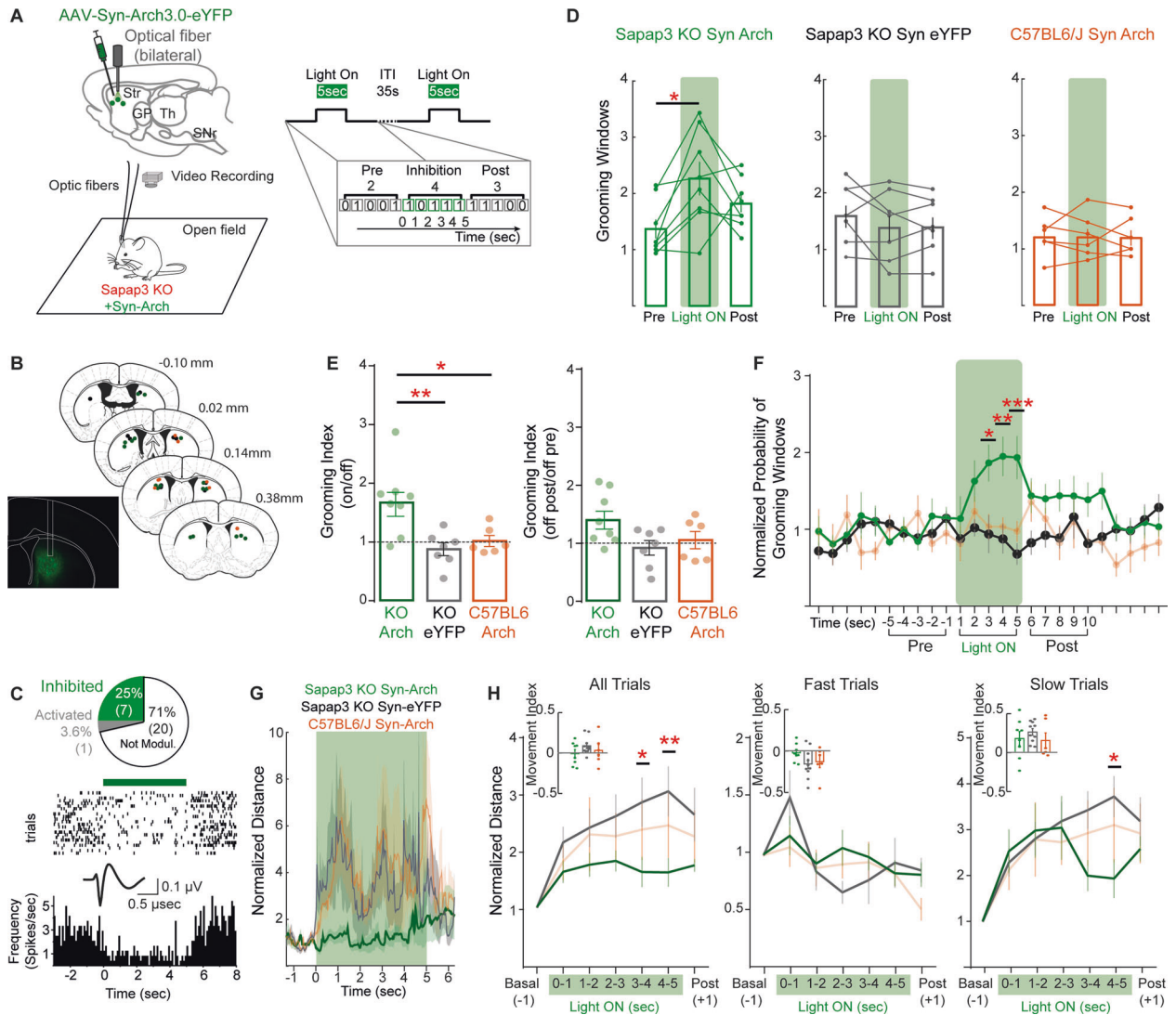


Fig. 4 Inhibition of striatal cells increases grooming behavior in Sapap3-KO mice. **A** Schematic diagram for surgery methodology, the open field setup, and the analysis method: The optogenetic effects were evaluated by the binary measure of 1 s windows that could contain grooming events for across the pre, inhibition and posterior periods. **B** Diagram showing the localization of the fiber optic tips in the DMS for Sapap3-KO Syn eYFP fiber tips; Orange dots: C57BL6/J Syn Arch fiber tips. **C** Raster plot of a representative unit recorded during the inhibition of striatal cells in a Sapap3-KO mouse. Insets: Upper panel, pie chart for the proportion of modulated cells. Lower panel, trace for the representative neuron in the raster plot. **D** Grooming Windows in each 5 s period for experimental and control groups (Sapap3-KO Syn Arch: 8 mice, Friedman Test $p < 0.01$, Dunn's multiple comparison $p < 0.05$; Sapap3-KO Syn eYFP: 7mice and C57BL6/J Syn Arch: 6 mice, Friedman Test $p > 0.05$, Dunn's multiple comparison $p > 0.05$). **E** Grooming Index for ON/OFF and OFF Post/ OFF Pre periods (Kruskal-Wallis with Dunn's multiple comparison, $*p < 0.05$, $**p < 0.01$). **F** Normalized Probability of Grooming Windows (Two-way ANOVA, $p < 0.001$, Post hoc Sidak $*p < 0.05$, $**p < 0.01$, $***p < 0.001$). **G** Example of the light pulse on the normalized displacement for each group (Mean \pm SE). **H** Quantification of the displacement normalized to 1 s before the start of the pulse for all, fast and slow trials (Two-Way ANOVA, Post Hoc Sidak $*p < 0.05$, $**p < 0.01$). Insets: Movement Index was calculated by dividing the mean of displacement during the 5 s pulse by the mean of displacement during the basal period.

has been shown during provocation of washing behaviors [54]. Our results suggest that the sustained activity of striatal cells during grooming series may be behind the maintenance of compulsive motor sequences.

Contrary to our hypothesis and, based on the activation of striatal cells during the onset of grooming events in the Sapap3-KO, inhibition of striatal activity increased the number of grooming bouts. One possible explanation is that interneurons play a key role in the regulation of striatal activity [55, 56]. Previous studies have suggested that parvalbumin interneurons contribute to the generation of compulsive responses [19, 24, 25]. Importantly, although no relationship between grooming and locomotion was observed in

the Sapap3-KO under no light inhibition, when inhibiting non-specific DMS neurons a relationship between these two parameters was observed: an increase in grooming corresponding to the seconds in which the locomotion was decreased. This suggests a possible relationship between these two parameters perhaps mediated by striatal activity. Note that in the control groups of the non-specific DMS inhibitions (Sapap3-KO eYFP and C57BL6/J Arch) neither grooming nor locomotion was affected.

The reduction in the grooming observed after the specific inhibition of indirect pathway striatal neurons could be explained in the light of studies looking at the effects of drugs used to treat compulsive behaviors in OCD patients. The principal

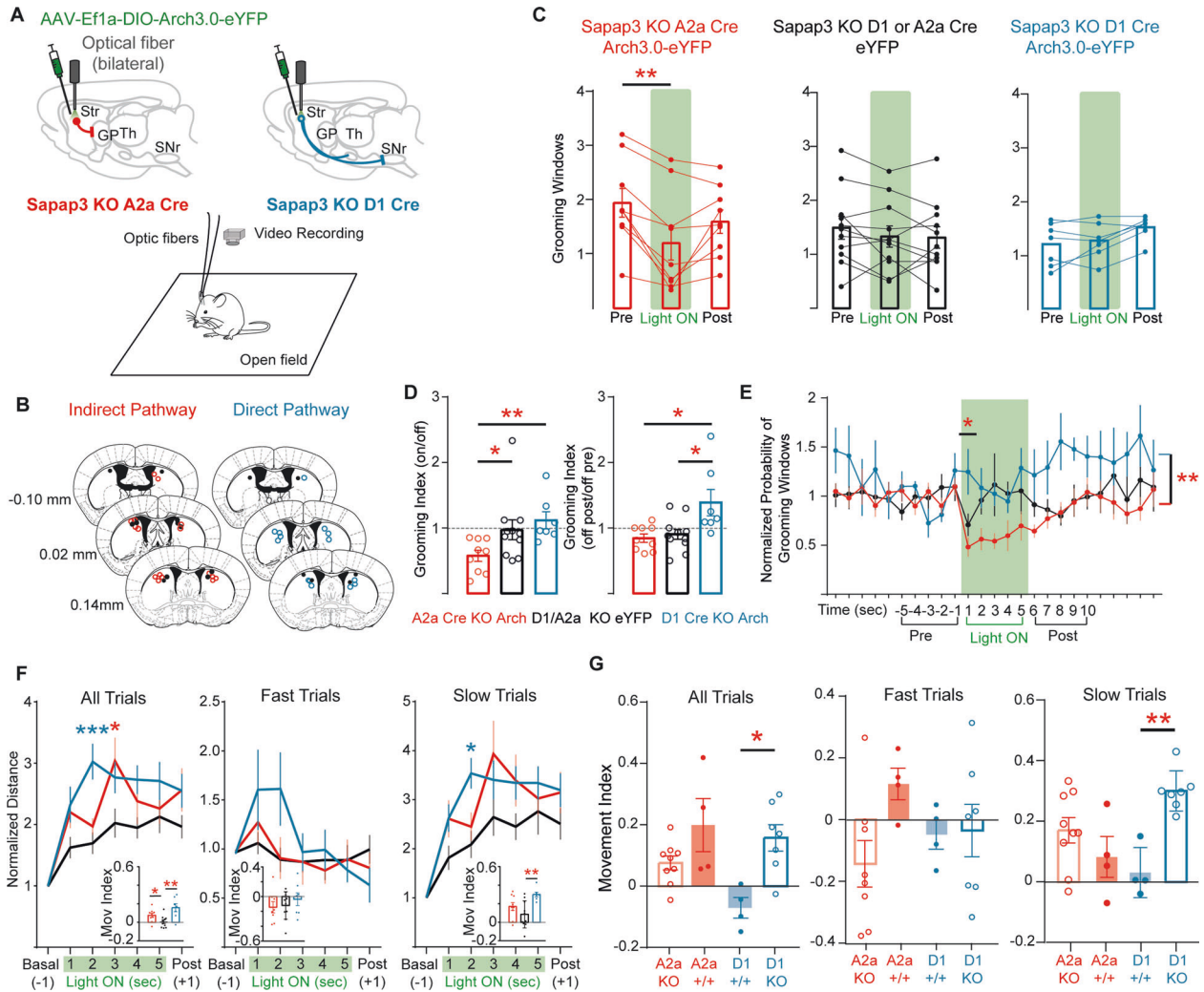


Fig. 5 Specific inhibition of indirect pathway neurons in the dorsolateral striatum decreases excessive grooming in the Sapap3-KO mice. **A** Schematic diagram for the two groups of animals generated to inhibit either the indirect (red) or the direct (blue) pathway striatal neurons in the open field setup. **B** Diagram for the localization of the fiber optic tips in the DMS for each group (Red dots: Sapap3-KO A2a Cre Arch-eYFP fiber tips; Blue dots: Sapap3-KO D1 Cre Arch-eYFP fiber tips; Black dots: Sapap3-KO A2a/D1 Cre eYFP fiber tips). **C** Grooming Windows in each 5 s period for experimental and control groups (A2a-Cre Sapap3-KO Arch: 9 mice; D1-Cre Sapap3-KO Arch: 7 mice; A2a/D1 Cre Sapap3 eYFP: 11 mice; Friedman Test $p < 0.01$, Dunn's multiple comparison $p < 0.01$). **D** Grooming Index for ON/OFF and OFF Post/ OFF periods (Kruskal-Wallis with Dunn's multiple comparison, $*p < 0.05$, $**p < 0.01$). **E** Normalized probability of grooming windows (Two-way ANOVA, $p < 0.01$, Post hoc Sidak $*p < 0.05$). **F** Quantification of the displacement normalized to 1 s before the start of the pulse for all, fast and slow trials (Two-Way ANOVA, Sidak Post Hoc $*p < 0.05$ and $***p < 0.001$). Insets: Movement Index: mean of displacement by second during the 5 s pulse/ the horizontal displacement during the second before the inhibition start. OFF for all, fast and slow trials (Mann-Whitney U, $*p < 0.05$ and $**p < 0.01$). **G** Comparison between movement index between A2a- or D1-Cre Sapap3-KO and A2a- or D1-Cre lines (Mann-Whitney U, $*p < 0.05$ and $**p < 0.01$).

pharmacology agents used to treat OCD are selective serotonin reuptake inhibitors (SSRI). Previous studies have shown that SSRIs, such as fluvoxamine, increase the availability of D2 receptors and D2/D3 binding affinity, which has been associated with treatment effectiveness [57, 58]. As D2 receptors are related to decreasing neuronal excitability and are used as a marker of indirect pathway neurons in the striatum [59], the reduction in grooming episodes observed during the inhibition of this pathway may explain in part the effects observed during OCD treatment. In addition, this pathway-specific contribution could be related to the fact that specific cortico-striatal deficits have been described in this model (e.g., alteration in the interaction of cortico-striatal inputs; [24, 25, 60]), perhaps specifically in indirect pathway neurons. fMRI studies have shown lateral orbitofrontal cortex (IOFC) activation during symptomatic provocation tasks in OCD patients [13, 60], and it has been suggested that the inhibition of striatal

activity by the activation of IOFC terminals reduces excessive grooming behavior in a classic conditioning paradigm [19]. In another study, striatal medium spiny neurons showed an increased response to the in-vitro optogenetic activation of M2 terminals in the striatum in the Sapap3-KO mice, which suggests a dysregulation of activity in the cortico-striatal circuit [24]. Further experiments are needed to elucidate the contribution of specific cortico-striatal loops to the generation of compulsive behaviors.

Finally, inhibition of direct pathway striatal neurons increased locomotion in Sapap3-KO but not wild-type animals, indicating that both striatal pathways are dysregulated in these mice. The altered cortico-striatal interactions reported in this model could impact on motor program selection processing which has been associated with the striatum [61, 62] and is suggested to be altered in OCD patients [63, 64]. Another explanation for the behavioral effects induced by optogenetic inhibition could be that

alterations to the neuronal firing frequency could disrupt pathological patterns in the striatum [65].

Overall, we conclude the Sapap3-KO mice present, in addition to an excessive grooming phenotype, decreased locomotion and smaller calcium events than their control littermates. Furthermore, optogenetic inhibition of the striatum (DMS) increases excessive grooming and reduces general locomotion in the Sapap3-KO. Only specific inhibition of striatopallidal neurons decreases the grooming phenotype observed in the Sapap3-KO mice. Importantly, specific inhibition of either the direct or the indirect pathway increases locomotion in the Sapap3 KO mice, suggesting a particular contribution of the latter in the control of locomotion in this model. The amelioration of the Sapap3-KO phenotypes (reduction excessive grooming and increased locomotion) by the inhibition of the indirect pathway suggests that the treatments that alleviate compulsive symptoms in OCD patients could exert their effects via this striatal population.

DATA AVAILABILITY

All data and MATLAB scripts will be made available by the lead or corresponding authors upon request.

REFERENCES

- Mushiake H, Inase M, Tanji J. Selective coding of motor sequence in the supplementary motor area of the monkey cerebral cortex. *Exp Brain Res*. 1990;82:208–210.
- DeLong MR. Primate models of movement disorders of basal ganglia origin. *Trends Neurosci*. 1990;13:281–5.
- Barnes TD, Kubota Y, Hu D, Jin DZ, Graybiel AM. Activity of striatal neurons reflects dynamic encoding and recoding of procedural memories. *Nature*. 2005;437:1158–61.
- Cui G, Jun SB, Jin X, Pham MD, Vogel SS, Lovinger DM, et al. Concurrent activation of striatal direct and indirect pathways during action initiation. *Nature*. 2014;494:238–42.
- Díaz-Hernández E, Contreras-López R, Sánchez-Fuentes A, Rodríguez-Sibrián L, Ramírez-Jarquín JO, Tecuapetla F. The thalamostriatal projections contribute to the initiation and execution of a sequence of movements. *Neuron*. 2018;100:739–52.
- American Psychiatric Association. *Diagnostic and statistical manual of mental disorders* (5th ed.). Washington, DC; 2013.
- Fava L, Bellantuono S, Bizzi A, Cesario ML, Costa B, De Simoni E, et al. Review of obsessive compulsive disorders theories. *Glob J Epidemiol Public Heal*. 2014;1:1–13.
- Rotge JY, Guehl D, Dilharreguy B, Tignol J, Bioulac B, Allard M, et al. Meta-analysis of brain volume changes in obsessive-compulsive disorder. *Biol Psychiatry*. 2009;65:75–83.
- Radua J, van den Heuvel OA, Surguladze S, Mataix-Cols D. Meta-analytical comparison of voxel-based morphometry studies in obsessive-compulsive disorder vs other anxiety disorders. *Arch Gen Psychiatry*. 2010;67:701–11.
- Shaw P, Sharp W, Sudre G, Wharton A, Greenstein D, Raznahan A, et al. Subcortical and cortical morphological anomalies as an endophenotype in obsessive-compulsive disorder. *Mol Psychiatry*. 2015;20:224–31.
- Breiter HC, Rauch SL, Kwong KK, Baker JR, Weisskoff RM, Kennedy DN, et al. Functional magnetic resonance imaging of symptom provocation in obsessive-compulsive disorder. *Arch Gen Psychiatry*. 1996;53:595–606.
- Lázaro L, Caldú X, Junqué C, Bargalló N, Andrés S, Morer A, et al. Cerebral activation in children and adolescents with obsessive-compulsive disorder before and after treatment: a functional MRI study. *J Psychiatr Res*. 2008;42:1051–9.
- Rotge J-Y, Guehl D, Dilharreguy B, Cuny E, Tignol J, Bioulac B, et al. Provocation of obsessive-compulsive symptoms: a quantitative voxel-based meta-analysis of functional neuroimaging studies. *J Psychiatry Neurosci*. 2008;33:405–12.
- Greer JM, Capecchi MR. Hoxb8 is required for normal grooming behavior in mice. *Neuron*. 2002;33:23–34.
- Welch JM, Lu J, Rodriguiz RM, Trotta NC, Peca J, Ding J-D, et al. Cortico-striatal synaptic defects and OCD-like behaviours in Sapap3-mutant mice. *Nature*. 2007;448:894–900.
- Shmelkov SV, Hormigo A, Jing D, Proenca CC, Bath KG, Milde T, et al. Slitrk5 deficiency impairs corticostriatal circuitry and leads to obsessive-compulsive-like behaviors in mice. *Nat Med*. 2010;16:598–602.
- Takeuchi M, Hata Y, Hirao K, Toyoda A, Irie M, Takai Y. SAPAPs. A family of PSD-95/SAP90-associated proteins localized at postsynaptic density. *J Biol Chem*. 1997;272:11943–51.
- Welch JM, Wang D, Feng G. Differential mRNA expression and protein localization of the SAP90/PSD-95-associated proteins (SAPAPs) in the nervous system of the mouse. *J Comp Neurol*. 2004;472:24–39.
- Burguière E, Monteiro P, Feng G, Graybiel AM. Optogenetic stimulation of lateral orbitofronto-striatal pathway suppresses compulsive behaviors. *Science*. 2013;340:1243–6.
- Mahgoub M, Adachi M, Suzuki K, Liu X, Kavalali ET, Chahrour MH, et al. MeCP2 and histone deacetylases 1 and 2 in dorsal striatum collectively suppress repetitive behaviors. *Nat Neurosci*. 2016;19:1506–12.
- Aldridge JW, Berridge KC, Rosen AR. Basal ganglia neural mechanisms of natural movement sequences. *Can J Physiol Pharmacol* 2004;82:732–9.
- Berridge KC, Whishaw IQ. Cortex, striatum and cerebellum: control of serial order in a grooming sequence. *Exp Brain Res*. 1992;90:275–90.
- Ahmari SE, Spellman T, Douglass NL, Kheirbek MA, Simpson HB, Deisseroth K, et al. Repeated cortico-striatal stimulation generates persistent OCD-like behavior. *Sci* (80-). 2013;340:1234–9.
- Corbit VL, Manning EE, Gittis AH, Ahmari SE. Strengthened inputs from secondary motor cortex to striatum in a mouse model of compulsive behavior. *J Neurosci*. 2019;39:2965–75.
- Hadjas LC, Schartner MM, Cand J, Creed MC, Pascoli V, Lüscher C, et al. Projection-specific deficits in synaptic transmission in adult Sapap3-knockout mice. *Neuropsychopharmacology*. 2020;45:2020–9.
- Ade KK, Wan Y, Hamann HC, O'Hare JK, Guo W, Quian A, et al. Increased metabotropic glutamate receptor 5 signaling underlies obsessive-compulsive disorder-like behavioral and striatal circuit abnormalities in mice. *Biol Psychiatry*. 2016;80:522–33.
- Glorie D, Verhaeghe J, Miranda A, Kertesz I, wyffels L, Stroobants S, et al. Progression of obsessive compulsive disorder-like grooming in Sapap3 knockout mice: a longitudinal [11C]ABP688 PET study. *Neuropharmacology*. 2020;177:108160.
- Ferré S, Karcz-Kubicha M, Hope BT, Popoli P, Burgueño J, Gutiérrez MA, et al. Synergistic interaction between adenosine A2A and glutamate mGlu5 receptors: implications for striatal neuronal function. *Proc Natl Acad Sci*. 2002;99:11940 LP–11945.
- Conn PJ, Battaglia G, Marino MJ, Nicoletti F. Metabotropic glutamate receptors in the basal ganglia motor circuit. *Nat Rev Neurosci*. 2005;6:787–98.
- Heintz N. Gene expression nervous system atlas (GENSAT). *Nat Neurosci*. 2004;7:483.
- Lopes G, Bonacchi N, Frazão J, Neto JP, Atallah BV, Soares S, et al. Bonsai: An Event-Based Framework for Processing and Controlling Data Stream. *Front Neuroinform*. 2015;9:1–14.
- Cai DJ, Aharoni D, Shuman T, Shobe J, Biane J, Song W, et al. A shared neural ensemble links distinct contextual memories encoded close in time. *Nature*. 2016;534:115–8.
- Schindelin J, Arganda-Carreras I, Frise E, Kaynig V, Longair M, Pietzsch T, et al. Fiji: an open-source platform for biological-image analysis. *Nat Methods*. 2012;9:676–82.
- Thevenaz P, Ruttimann UE, Unser M. A pyramid approach to subpixel registration based on intensity. *IEEE Trans Image Process*. 1998;7:27–41.
- Lu J, Li C, Singh-Alvarado J, Zhou ZC, Fröhlich F, Mooney R, et al. MIN1PIPE: a microscope 1-photon-based calcium imaging signal extraction pipeline. *Cell Rep*. 2018;23:3673–84.
- Pnevmatikakis EA, Soudry D, Gao Y, Machado TA, Merel J, Pfau D, et al. Simultaneous denoising, deconvolution, and demixing of calcium imaging data. *Neuron*. 2016;89:285–99.
- Sheintuch L, Rubin A, Brande-Eilat N, Geva N, Sadeh N, Pinchasof O, et al. Tracking the same neurons across multiple days in Ca2+ imaging data. *Cell Rep*. 2017;21:1102–15.
- Hadjas LC, Lüscher C, Simmler LD. Aberrant habit formation in the Sapap3-knockout mouse model of obsessive-compulsive disorder. *Sci Rep*. 2019;9:12061.
- van den Boom BJG, Mooij AH, Misevičiūtė I, Denys D, Willuhn I. Behavioral flexibility in a mouse model for obsessive-compulsive disorder: impaired pavlovian reversal learning in SAPAP3 mutants. *Genes Brain Behav*. 2019;18:12557–12557.
- Ehmer I, Feenstra M, Willuhn I, Denys D. Instrumental learning in a mouse model for obsessive-compulsive disorder: Impaired habit formation in Sapap3 mutants. *Neurobiol Learn Mem*. 2020;168:107–62.
- Aldridge JW and Berridge KC. Coding of Serial Order by Neostriatal Neurons: A "Natural Action" Approach to Movement Sequence. *J Neurosci*. 1998;18:2777–2787.
- Kalueff AV, Stewart AM, Song C, Berridge KC, Graybiel AM, Fentress JC. Neurobiology of rodent self-grooming and its value for translational neuroscience. *Nat Rev Neurosci*. 2015;17:45–59.
- Albin RL, Young AB, Penney JB. The functional anatomy of basal ganglia disorders. *Trends Neurosci*. 1989;12:366–75.

44. Redgrave P, Vautrelle N, Reynolds JNJ. Functional properties of the basal ganglia's re-entrant loop architecture: Selection and reinforcement. *Neuroscience*. 2011;198:138–51.
45. Kravitz AV, Freeze BS, Parker PRL, Kay K, Thwin MT, Deisseroth K, et al. Regulation of parkinsonian motor behaviours by optogenetic control of basal ganglia circuitry. *Nature*. 2010;466:622–6.
46. Manning EE, Dombrovski AY, Torregrossa MM, Ahmari SE. Impaired instrumental reversal learning is associated with increased medial prefrontal cortex activity in Sapap3 knockout mouse model of compulsive behavior. *Neuropsychopharmacol. Publ Am Coll Neuropsychopharmacol*. 2019;44:1494–504.
47. Boom BJJ, Van Den, Mooij AH, Misevičiūtė I, Denys D. Behavioral flexibility in an OCD mouse model: Impaired Pavlovian reversal learning in SAPAP3 mutants. *Genes Brain Behav*. 2019;18:12557–12557.
48. Chen M, Wan Y, Ade K, Ting J, Feng G, Calakos N. Sapap3 deletion anomalously activates short-term endocannabinoid-mediated synaptic plasticity. *J Neurosci*. 2011;31:9563–73.
49. Wan Y, Feng G, Calakos N. Sapap3 deletion causes mGluR5-dependent silencing of AMPAR synapses. *J Neurosci*. 2011;31:16685 LP–16691.
50. Matamales M, Götz J, Bertran-Gonzalez J. Quantitative imaging of cholinergic interneurons reveals a distinctive spatial organization and a functional gradient across the mouse striatum. *PLoS One*. 2016;11:e0157682.
51. Yin HH, Knowlton BJ, Balleine BW. Inactivation of dorsolateral striatum enhances sensitivity to changes in the action-outcome contingency in instrumental conditioning. *Behav Brain Res*. 2006;166:189–96.
52. Matamales M, McGovern AE, Mi JD, Mazzone SB, Balleine BW, Bertran-Gonzalez J. Local D2- to D1-neuron transmodulation updates goal-directed learning in the striatum. *Sci (80-)*. 2020;367:549 LP–555.
53. Rauch SL, Jenike MA, Alpert NM, Baer L, Breiter HCR, Savage CR, et al. Regional cerebral blood flow measured during symptom provocation in obsessive-compulsive disorder using oxygen 15—labeled carbon dioxide and positron emission tomography. *Arch Gen Psychiatry*. 1994;51:62–70.
54. Mataix-Cols D, Wooderson S, Lawrence N, Brammer MJ, Speckens A, Phillips ML, et al. Distinct neural correlates of washing, checking, and hoarding symptom dimensions in obsessive-compulsive disorder. *Arch Gen Psychiatry*. 2004;61:564–76.
55. Silberberg G, Bolam JP. Local and afferent synaptic pathways in the striatal microcircuitry. *Curr Opin Neurobiol*. 2015;33:182–7.
56. Tepper JM, Koós T, Ibanez-Sandoval O, Tecuapetla F, Faust TW, Assous M. Heterogeneity and diversity of striatal GABAergic interneurons: update 2018. *Front Neuroanat*. 2018;12:91.
57. Moresco RM, Pietra L, Henin M, Panzacchi A, Locatelli M, Bonaldi L, et al. Fluvoxamine treatment and D2 receptors: a pet study on OCD drug-naïve patients. *Neuropsychopharmacology*. 2007;32:197–205.
58. Ducasse D, Boyer L, Michel P, Loundou A, Macgregor A, Micoulaud-Franchi J-A, et al. D2 and D3 dopamine receptor affinity predicts effectiveness of antipsychotic drugs in obsessive-compulsive disorders: a metaregression analysis. *Psychopharmacol*. 2014;231:3765–70.
59. Surmeier DJ, Song WJ, Yan Z. Coordinated expression of dopamine receptors in neostriatal medium spiny neurons. *J Neurosci*. 1996;16:6579–91.
60. Simon D, Kaufmann C, Müsch K, Kischkel E, Kathmann N. Fronto-striato-limbic hyperactivation in obsessive-compulsive disorder during individually tailored symptom provocation. *Psychophysiology*. 2010;47:728–38.
61. Kim HF, Amita H, Hikosaka O. Indirect pathway of caudal basal ganglia for rejection of valueless visual objects. *Neuron*. 2017;94:920–30.
62. Schmidt R, Leventhal DK, Mallet N, Chen F, Berke JD. Canceling actions involves a race between basal ganglia pathways. *Nat Neurosci*. 2013;16:1118–24.
63. Saxena S, Bota RG, Brody AL. Brain-behavior relationships in obsessive-compulsive disorder, in seminars in clinical. *Neuropsychiatry*. 2001;6:82–101. pp.
64. Ahmari SE, Dougherty DD. Dissecting OCD circuits: from animal models to targeted treatments. *Depress Anxiety*. 2015;32:550–62.
65. Grover S, Nguyen JA, Viswanathan V, and Reinhart RMG. High-frequency neuro-modulation improves obsessive-compulsive behavior. *Nat. Med*. 2021;27:232–8.

ACKNOWLEDGEMENTS

We thank Professor Dr. Rui Costa for the D1- and A2a-Cre mice. PhD Catherine French for proofreading of the manuscript. The IFC-Animal Facilities and the Imaging units.

AUTHOR CONTRIBUTIONS

KIR-A and FT designed and wrote the study. KIR-A and HA-L performed the acquisition of the calcium recordings. HA-L performed the recordings of electrophysiology signal events. AKV-R configured the miniscope acquisition system. JOR-J provided the genotyping and technical support for the development of the study. AL-M performed the optogenetic inhibition of C57BL/6J A2a- and D1-Cre mice. KIR-A analyzed the calcium signals and electrophysiological recordings and performed the Sapap3, Sapap3 A2a-Cre, and Sapap3 D1-Cre optogenetic inhibitions.

FUNDING

KIR-A is a doctoral student of Programa de Doctorado en Ciencias Bioquímicas, Universidad Nacional Autónoma de México (UNAM) and was supported by the fellowship 584044 from CONACYT. This work was supported by the Ciencia Básica CONACyT grant 220412, Fronteras de la Ciencia CONACyT grants 2022 and 154039, the DGAPA-PAPIIT-UNAM grants IA200815, IN226517, IN203420 and the Moshinsky fellowship to FT.

COMPETING INTERESTS

The authors declare no competing interests.

ADDITIONAL INFORMATION

Supplementary information The online version contains supplementary material available at <https://doi.org/10.1038/s41386-021-01161-9>.

Correspondence and requests for materials should be addressed to F.T.

Reprints and permission information is available at <http://www.nature.com/reprints>

Publisher's note Springer Nature remains neutral with regard to jurisdictional claims in published maps and institutional affiliations.